View metadata, citation and similar papers at core.ac.uk

brought to you by CORE

provided by NASA Technical Reports Server

NASA-TM-111578

# Hover Acoustic Characteristics of the XV-15 with Advanced Technology Blades

D. A. Conner and J. B. Wellman

Reprinted from

Journal of Aircraft

Volume 31, Number 4, Pages 737–744

A publication of the
American Institute of Aeronautics and Astronautics, Inc.
370 L'Enfant Promenade, SW
Washington, DC 20024-2518

JOURNAL OF AIRCRAFT
Vol. 31, No. 4, July–Aug. 1994

# Hover Acoustic Characteristics of the XV-15 with Advanced Technology Blades

David A. Conner*
*NASA Langley Research Center, Hampton, Virginia 23681*
and
J. Brent Wellman†
*NASA Ames Research Center, Moffett Field, California 94035*

**An experiment has been performed to investigate the far-field hover acoustic characteristics of the XV-15 aircraft with advanced technology blades (ATB). An extensive, high-quality, far-field acoustics data base was obtained for a rotor tip speed range of 645–771 ft/s. A 12-microphone, 500-ft radius semicircular array combined with two aircraft headings provided acoustic data over the full 360-deg azimuth about the aircraft with a resolution of 15 deg. Altitude variations provided data from near in-plane to 45 deg below the rotor tip path plane. Acoustic directivity characteristics in the lower hemisphere are explored through pressure time histories, narrow-band spectra, and contour plots. Directivity patterns were found to vary greatly with azimuth angle, especially in the forward quadrants. Sharp positive pressure pulses typical of blade-vortex interactions were found to propagate aft of the aircraft and were most intense at 45 deg below the rotor plane. Modest overall sound pressure levels were measured near in-plane indicating that thickness noise is not a major problem for this aircraft when operating in the hover mode with ATB. Rotor tip speed reductions reduced the average overall sound pressure level [dB (0.0002 dyne/cm²)] by nearly 8 dB in-plane, and by almost 5 dB at 12.6 deg below the rotor plane.**

## Nomenclature

$V_t$ = rotor blade tip speed, ft/s
$\theta$ = angle below the rotor tip path plane, deg
$\Psi$ = azimuth angle about the aircraft, deg (0-deg aft)

## Introduction

AIR traffic congestion at major airports throughout the world is quickly reaching the saturation point. The economic and political difficulties of constructing new major airports in heavily populated areas are enormous. Smaller commuter aircraft account for approximately 30% of airport usage while carrying only 5% of the passengers. A civil tiltrotor commuter transport, therefore, offers a potential solution for relieving this air traffic congestion. A fleet of civil tiltrotor transports, operating in a National Airspace System tailored to permit vertiport access independent of airport control, would permit a significant increase in airport passenger movements.

A potential problem with operating the tiltrotor aircraft in highly populated areas is unacceptably high noise levels on approach and departure and while performing terminal area operations. While operating in airplane mode, the tiltrotor aircraft is very quiet. However, while operating in tiltrotor mode or in helicopter mode, as would be required near vertiports, the noise levels are at least comparable to helicopters of similar gross weights.

Previous noise studies on the XV-15 tiltrotor aircraft have been limited. A brief 1981 hover noise test conducted at Moffett Field, CA, found that the noise levels radiated aft of the aircraft were slightly higher than the forward radiated noise levels.[1] Flight tests conducted at Crow's Landing, CA, in 1982 and in 1986 obtained acoustic data for level flight conditions and for approaches at several glideslopes.[2] All acoustic results reported from both the aforementioned tests were obtained from microphones mounted on 4-ft stands. A 1988 flight test conducted at Maypearl, TX, obtained acoustic measurements for level flight conditions and for normal and noise-abatement approaches and departures. Acoustic data from this test were obtained from ground-board mounted microphones,[3] as well as from microphones mounted on 4-ft stands.[4] Wind-tunnel acoustic data were obtained during a full-scale test of the XV-15 in the Ames 40- by 80-ft Wind Tunnel.[5]

A limited amount of analytical noise prediction work has been done for tiltrotors. A study of hover noise prediction methods with emphasis on the fountain flow effect (recirculation of the rotor downwash caused by wing blockage) is presented in Ref. 6. Reference 7 reviews the state of knowledge and the needed improvement in noise methodology and measurements for tiltrotor aircraft, while Ref. 8 reviews the background of U.S. tiltrotor development and key issues for civil tiltrotor applications with special attention to noise considerations for civil tiltrotor operations. In addition, current research and technology development efforts at the Langley Research Center are reviewed and future research needs are identified in Ref. 8.

One important aspect of terminal area operations is hover. To obtain a better understanding of the hover acoustic characteristics of a tiltrotor aircraft, acoustic hover tests were conducted on a XV-15 tiltrotor aircraft with advanced technology blades (ATB). The purpose of the test program was to obtain a comprehensive data base of far-field hover acoustics for the XV-15/ATB tiltrotor aircraft (tail number 703) for a range of rotor tip speeds and wheel heights. The tests were conducted at NAS Moffett Field, CA, on December 5–7, 1990.

This article presents a description of the data systems, instrumentation accuracies, and experimental test techniques utilized for this test program. The acoustic directivity char-

Received Feb. 16, 1992; revision received May 27, 1993; accepted for publication May 27, 1993. This paper is declared a work of the U.S. Government and is not subject to copyright protection in the United States.

*Rotorcraft Acoustics Engineer, Joint Research Program Office, AeroFlightDynamics Directorate, ARDEC, ATCOM, Applied Acoustics Branch, Acoustics Division. Senior Member AIAA.

†XV-15 Research Team Leader, AeroFlightDynamics Directorate, ARDEC, ATCOM, Flight Experiments Branch, Aircraft Technology Division.

acteristics in the lower hemisphere, from in-plane to 45 deg below the rotor tip-path-plane, are explored using pressure time histories, narrow-band spectra, and contour plots of the overall sound pressure level (OASPL) and the sound pressure level (SPL) [dB (0.0002 dyne/cm$^2$)] of the fundamental blade passage frequency. In addition, the effects of rotor tip speed reductions on the level and character of the acoustic signature are investigated through time and frequency domain analyses.

## Description of Experiment

### Test Aircraft

The XV-15 (Fig. 1) is a proof-of-concept demonstrator aircraft.[9] It features twin rotor systems mounted on pivoting nacelles at the ends of its swept-forward wings. These nacelles are tilted into the vertical position for vertical takeoffs and landings and rotated to the horizontal for cruising flight. Two of these aircraft were built.

The XV-15 used in this flight test was fitted with the ATB[10] rotor system designed specifically for higher operating weights and improved maneuver load factors in helicopter and transition modes of operation. The ATB feature fiberglass and carbon composite honeycomb construction, advanced thin airfoil sections, and a highly pronounced nonlinear thickness distribution. Rotor solidity was increased over the standard metal blades to provide greater rotor thrust over a larger rotor rpm range. Untwisted blade planform drawings of the ATB and the original metal blades are provided in Fig. 2. The outer 10% of the blades were removable for tip studies; however, due to structural problems with the twisted blade tips, only the alternate untwisted tips were used for this test. Acoustic considerations of the ATB design included the use of very thin airfoil sections for the reduction of thickness noise and a high thrust level at low rpm allowing for reduced tip speed operations.

The XV-15 features an impressive on-board suite of instrumentation. Transducers include strain gauges, temperature sensors, accelerometers, rate sensors, and pressure transducers. Data from these transducers are forwarded to three remote multiplexer-demultiplexer units which provide signal conditioning, digitization, and encoding into pulse-coded modulation format. The data stream is then recorded on an on-board tape recorder and transmitted to the ground using L-band telemetry for recording on a ground-based incident tape. A time correlation base for this system is supplied in IRIG-B format by an on-board time code generator synchronized to a GOES satellite prior to each flight.

Two push button switches are provided to the crew members to provide a coded mark on the data tape to designate "prime data." When prime data is activated, all transducer scans are initiated and end when prime data is deactivated. Prime data numbers reference certain segments of the data stream and associate them with flight conditions or specific states of the aircraft. As such, they provide vital identification of data for inclusion in the tiltrotor engineering database system (TRENDS).[11]

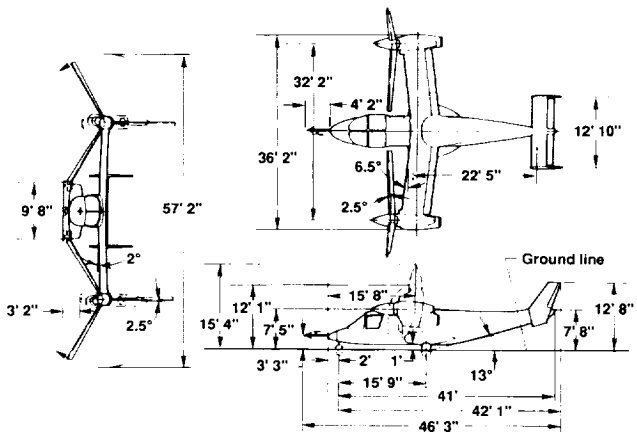


Fig. 1 XV-15 tiltrotor research aircraft.

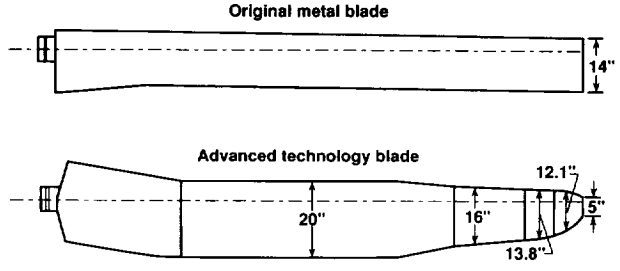


Fig. 2 Untwisted rotor blade planform drawings.

### Meteorological Instrumentation

Two data systems were used to acquire weather information: 1) a weather balloon system and 2) a weather profiler system. The weather balloon system, located approximately 1400 ft SSW of the hover point (see Fig. 3), consisted of an electric winch-controlled, tethered, helium-filled balloon, an instrument/telemetry pod, a ground-based receiver/data-controller, and a ground-based support computer. Profiles of temperature, relative humidity, wind speed, and wind direction were acquired up to 1000-ft altitude before, during, and after flight testing. The weather profiler system, located approximately 1300 ft WNW of the hover point (see Fig. 3), consisted of a 10-m tower with 10 temperature sensors, 5 anemometers, and 3 wind direction sensors. The weather profiler was used to obtain detailed weather information near the ground. Weather data from both systems were acquired at a rate of 6 points per minute, displayed in real time, and recorded, along with satellite time code, on a magnetic disk.

### Acoustic Instrumentation

The acoustic instrumentation consisted of 12 microphone systems operated from one mobile data van. Each microphone system consisted of a $\frac{1}{2}$-in. omnidirectional condenser microphone (B & K 4134) fitted with a grid cap and wind screen and mounted on its own planar ground-board, a preamplifier/heater, a power supply/line driver, and an amplifier. The microphones were deployed in a 500-ft radius semicircular array, centered on the hover point, with microphones located at every 15 deg of azimuth as shown in Fig. 3. Each microphone signal was recorded, along with satellite time code, on a frequency-modulated, 14-track wideband-I analog tape recorder operating at 15 in./s, thus providing a maximum frequency capability of 10,000 Hz. A pistonphone was used in

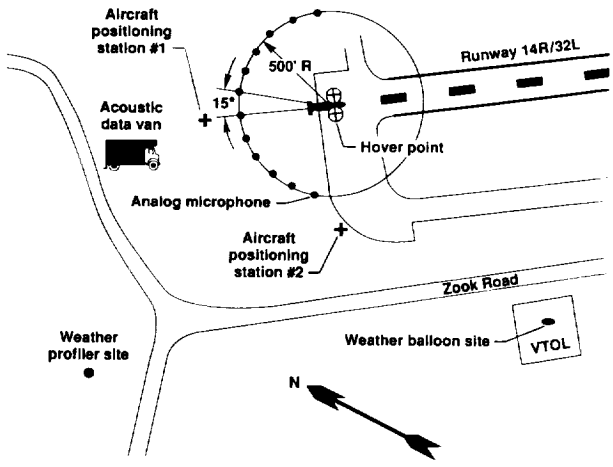


Fig. 3 XV-15/ATB far-field hover acoustics test set-up at Moffett Field, CA.

the field each day before and after flight testing for sound level calibration.

#### Flight Test Procedures and Stationkeeping

At the time of the test, the ATB initial envelope expansion program had not been completed. The XV-15 was, therefore, confined to the airspace of the Naval Air Station, Moffett Field, contiguous with Ames Research Center. When conducting acoustic tests, it is desirable to have low ambient noise levels; therefore, much effort was expended to coordinate with the U.S. Navy, NASA, and several surrounding agencies, companies, and local governments to establish a "quiet time" during the test periods when high level noise sources were silenced and activity was kept to a minimum.

The specific location for the test was at the end of the shorter of two parallel runways. The acoustic array was centered on the apex of a chevron mark on the north end of the runway apron. The runway centerline provided a good alignment cue for the crew while hovering. Additional positioning was provided by two positioning stations (Fig. 4) located on the extended centerline of the runway and at right angles to the centerline. Team engineers equipped with surveyors' transits radioed correction information to the crew. By sighting on the aircraft's main landing gear and keeping it within the transit stadia marks, the team was assured that the aircraft was within $\pm 6$ ft of the intended point in space in all directions. Acoustic data about the entire azimuth of the aircraft were obtained by hovering the aircraft above the center of the semicircular microphone array with a heading of 140 deg and then immediately repeating the run with an aircraft heading of 320 deg. For this article, $\theta$ is calculated as the arc tangent of the prescribed altitude plus 12 ft (to account for the distance from the landing gear to the rotor plane), divided by the array radius.

## Data Reduction and Analysis

Acoustic data were processed into pressure time histories and narrow-band spectra. Initial inspection of narrow-band spectra for the full 10-kHz bandwidth available showed that the vast majority of the acoustic energy was contained below 2 kHz. In addition, most data obtained beyond 2 kHz were significantly below the maximum levels, approaching the maximum dynamic range of the recording system (ideally 48 dB). For these reasons, and to more closely study the lower frequency tonal content of the measured acoustic signals, each acoustic record was low-pass filtered at 2 kHz and digitized at a rate of 4096 samples per second. For the narrow-band analysis, the data were divided into 40 consecutive, nonoverlapping blocks of 2048 points each, a Hamming data window was applied, and a spectrum was calculated for each block. Each of these 40 spectra was then averaged to provide a spectrum that has a 90% confidence level in the amplitude estimates with an interval of $-1.4$ to 1.8 dB based on a chi-square distribution. The bandwidth of the narrow-band analysis was 2 Hz.

Fig. 4 Aircraft positioning station no. 1.

## Results and Discussion

Acoustic data were obtained on 3 consecutive days between the hours of 0700 (dawn) and 0800, due to the optimal (minimum) wind conditions which typically occur at this time of day. Soon after dawn the winds generally increase due to the temperature inversion which develops as the sun heats the ground. During this test program, the winds were generally less than 2 mph at ground level and increased to 5 mph at 500-ft altitude. Above 500 ft, the winds increased to as much as 20 mph at 1000-ft altitude. The wind direction was typically out of the NNW at ground level and shifted to the N to NNE at 500-ft altitude. Examples of weather profiles obtained during this test program are presented in Fig. 5.

#### Data Repeatability

To determine the repeatability of data obtained during this test program, the first data run each morning was conducted at identical aircraft operating conditions of 100-ft altitude and 98% rpm ($V_t$ = 771 ft/s). Polar plots of the OASPL and the SPL of the fundamental blade passage frequency, (BPF) as a function of $\Psi$ for these three runs are presented in Fig. 6. Figure 6a shows that the maximum difference in the OASPL at any azimuth angle is 3 dB. The maximum difference in the SPLs of the fundamental BPF (Fig. 6b), with the exception of 5 of the 24 measurement locations ($\Psi$ = 75, 165, 195, 225, and 345 deg), is also less than 3 dB. This is within the spectral

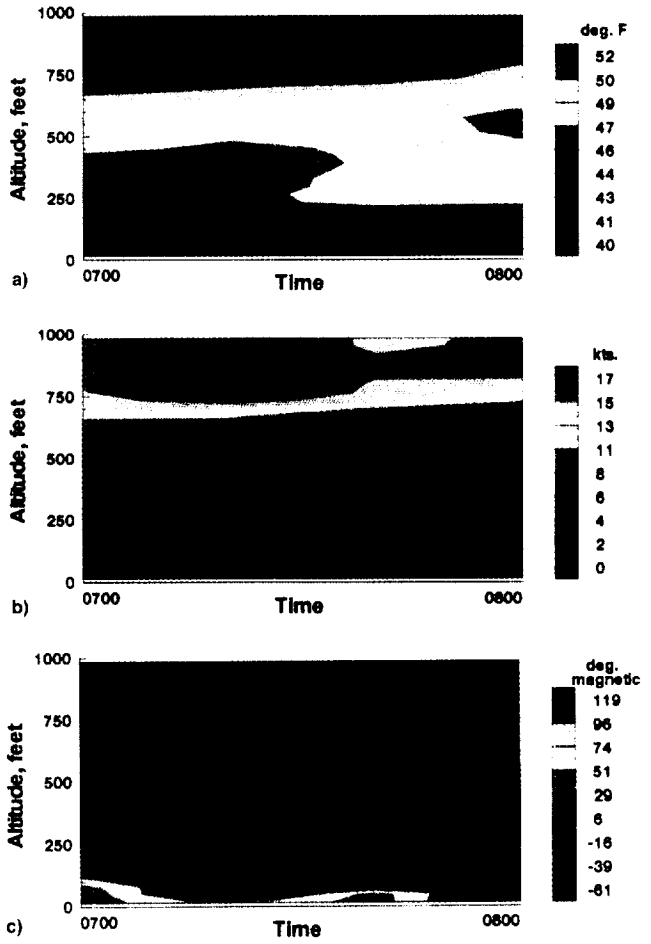


Fig. 5 Weather profiles at Moffett Field, CA, December 6, 1990: a) temperature, b) wind speed, and c) wind direction.

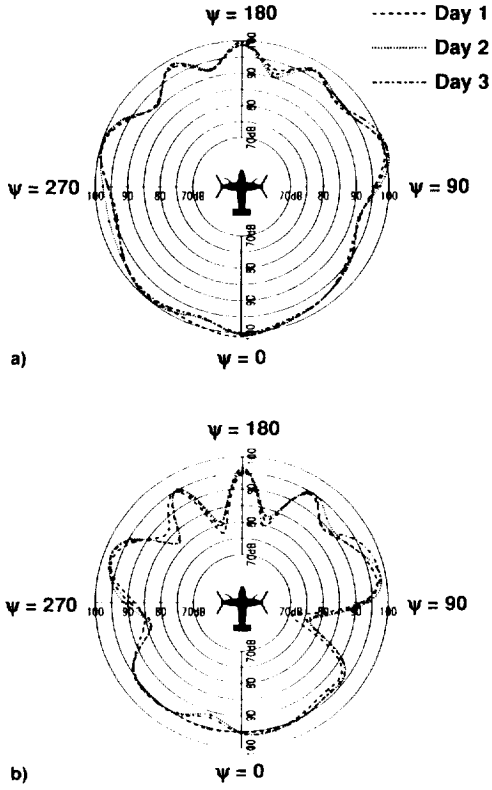


Fig. 6 Data repeatability study; $\theta$ = 12.6 deg, $V_t$ = 771 ft/s: a) OASPL and b) fundamental BPF.

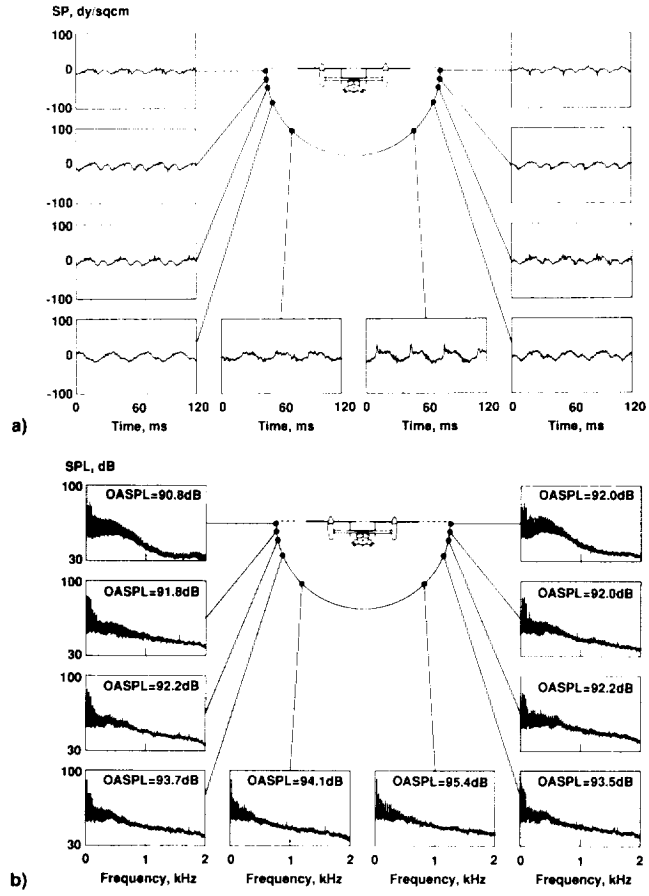


Fig. 7 Hover acoustic characteristics about the XV-15 aircraft lateral axis; $V_t$ = 771 ft/s, effective microphone distance = 715 ft: a) pressure time histories and b) narrow-band spectra.

estimate error bounds of −1.4 to 1.8 dB. The maximum difference in the SPL of the fundamental BPF was approximately 5 dB and occurred at $\Psi$ = 225 deg. This figure indicates that the data obtained during this flight test program, though highly variable with azimuth angle, are very repeatable and lends confidence that the data are of high quality.

### Acoustic Characteristics

Pressure time histories and narrow-band spectra about the aircraft longitudinal or roll axis at $\Psi$ = 90 and 270 deg for a rotor tip speed of 771 ft/s and a gross weight range of 13,000–13,500 lb are presented in Fig. 7. All data were corrected to a 715-ft distance (assuming spherical spreading), which is the distance from the aircraft to the microphone array for the 500-ft altitude runs. Data are presented at 1.6, 7.1, 12.6, 23.0, and 45.7 deg below the rotor tip path plane. The pressure time histories of Fig. 7a present 120 ms of data, or slightly more than one rotor revolution. The pressure time histories on either side of the aircraft are very similar in waveform and magnitude. The effect of changes in the relative phase angles of the acoustic signals for the two rotor systems with altitude due to changes in the relative rotor-to-microphone distances is evident in the waveforms as the two signals combine constructively and destructively (i.e., 6 humps at $\theta$ = 7.1 deg, 3 humps at $\theta$ = 23 deg). The narrow-band spectra presented in Fig. 7b show a richer harmonic content for the in-plane acoustic data, probably due to the dominance of rotor thickness noise. The OASPL increases by slightly more than 3 dB as $\theta$ increases from 1.6 to 45.7 deg with the greatest increase (approximately 1.5 dB) occurring as $\theta$ increases from 12.6 to 23 deg. The OASPL for the out-of-plane data are dominated by the lower harmonics (loading noise), whereas the higher harmonic content typical of thickness noise contributes more to the OASPL for the in-plane data. Inspection of ambient noise data obtained immediately prior to and following the test periods showed that the background noise levels were significantly less than the measured aircraft noise levels for all frequencies. The background noise levels were typically between 55–60 dB at about 20 Hz and fall off rapidly to below 30 dB above 200 Hz.

All acoustic data presented in this article were obtained with the aircraft operating out of ground effects with the exception of the data presented for $\theta$ = 1.6 deg, which were obtained with the aircraft operating at a rotor height of 14 ft. In addition to the increased lift provided by ground effects, a change in the recirculation characteristics may also be occurring near the ground. Increased lift due to ground effects should not significantly alter the data presented for $\theta$ = 1.6 deg since these in-plane data are dominated by blade thickness noise. Also, aircraft state data show that the rotor collective settings did not change significantly when hovering in and out of ground effects. Changes in the recirculation characteristics, however, are not known at this time and the reader needs to consider this unknown factor when interpreting these results.

Pressure time histories and narrow-band spectra about the aircraft lateral or pitch axis at $\Psi$ = 0 and 180 deg for the same rotor tip speed of 771 ft/s and gross weight range of 13,000–13,500 lb are presented in Fig. 8. As with the data of Fig. 7, these data have been corrected to a distance of 715 ft. The phase angles for the acoustic data from the two rotor systems are equal at all altitudes for the azimuth angles presented in this figure; therefore, only 3 humps per rotor revolution are present. The pressure time histories of Fig. 8a show a drastic difference in the waveforms propagated forward and aft of the aircraft. The sharp positive pressure pulses which exist in the acoustic data aft of the aircraft are typical of a blade-vortex interaction type noise. It is believed that this is due to rotor interaction with the turbulent "fountain flow" (see Ref. 6) created as the rotor downwash impacts the wing and is recirculated back through the rotors over the inboard portion of the wing. These sharp positive pressure

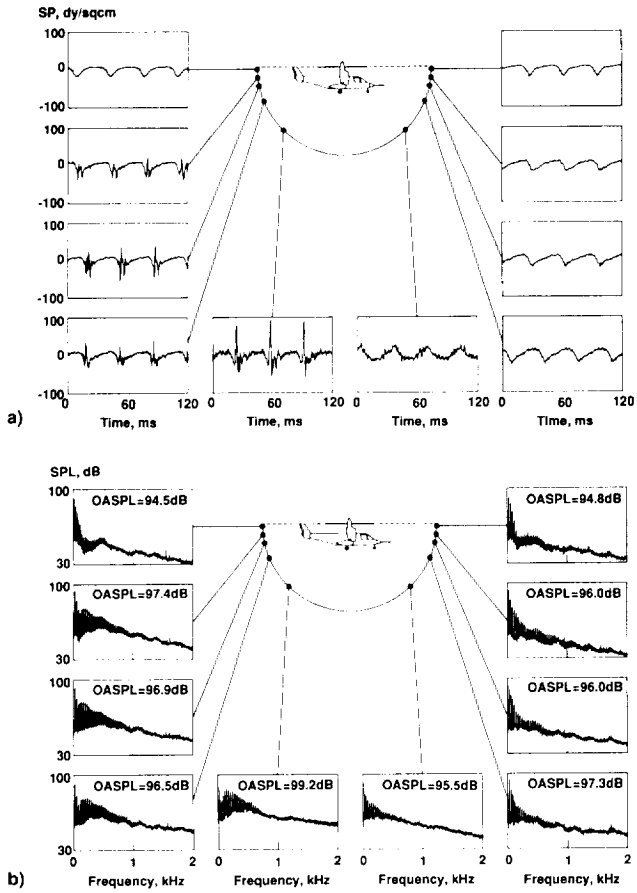


**Fig. 8 Hover acoustic characteristics about the XV-15 aircraft longitudinal axis; $V_T$ = 771 ft/s, effective microphone distance = 715 ft: a) pressure time histories and b) narrow-band spectra.**

pulses do not exist in the acoustic data measured in front of the aircraft. This is due to the direction of rotation of the rotors (clockwise on the port side and counterclockwise on the starboard side). Because the rotor blades impact the turbulent fountain flow while moving in a rearward direction, the impulsive noise is propagated toward the rear of the aircraft. The impulsive character of the pressure time histories can be seen in the narrow-band spectra of Fig. 8b as richer harmonic content for frequencies up to approximately 1000 Hz. Minimum OASPLs were measured in-plane while the maximum OASPL was measured aft of the aircraft at $\theta$ = 45.7 deg.

Pressure time histories about the aircraft at $\theta$ = 1.6, 12.6, and 45.7 deg for the maximum rotor tip speed of 771 ft/s and a gross weight range of 13,000–13,500 lb are presented in Figs. 9a–9c, respectively. These data have been corrected to an equal source-to-microphone distance of 715 ft. Each pressure time history represents 120 ms of data, or approximately one rotor revolution, with a vertical or pressure scale of −90 to +140 dynes/cm$^2$. Figure 9a shows that, acoustically, there is nothing of special interest occurring at $\theta$ = 1.6 deg for any azimuth angle. At $\theta$ = 12.6 deg, however, Fig. 9b shows that the blade-vortex interaction (BVI) type interactions that were seen in Fig. 8 at $\Psi$ = 0 deg are beginning to occur in the rear quadrants from $\Psi$ = 300 to 45 deg. BVI is much more intense in the data at $\theta$ = 45.7 deg from $\Psi$ = 270 to 75 deg (Fig. 9c). BVI intensity is maximum at $\Psi$ = 0 deg and decreases as you move forward on either side of the aircraft. In addition, data for all azimuth angles at $\theta$ = 45.7 deg contain a higher level of high-frequency noise compared to Figs. 9a and 9b. This is probably rotor broadband noise, which propagates minimally in-plane.

Lower hemispherical contour plots of the OASPL and the fundamental BPF, from in-plane to 45 deg below the rotor

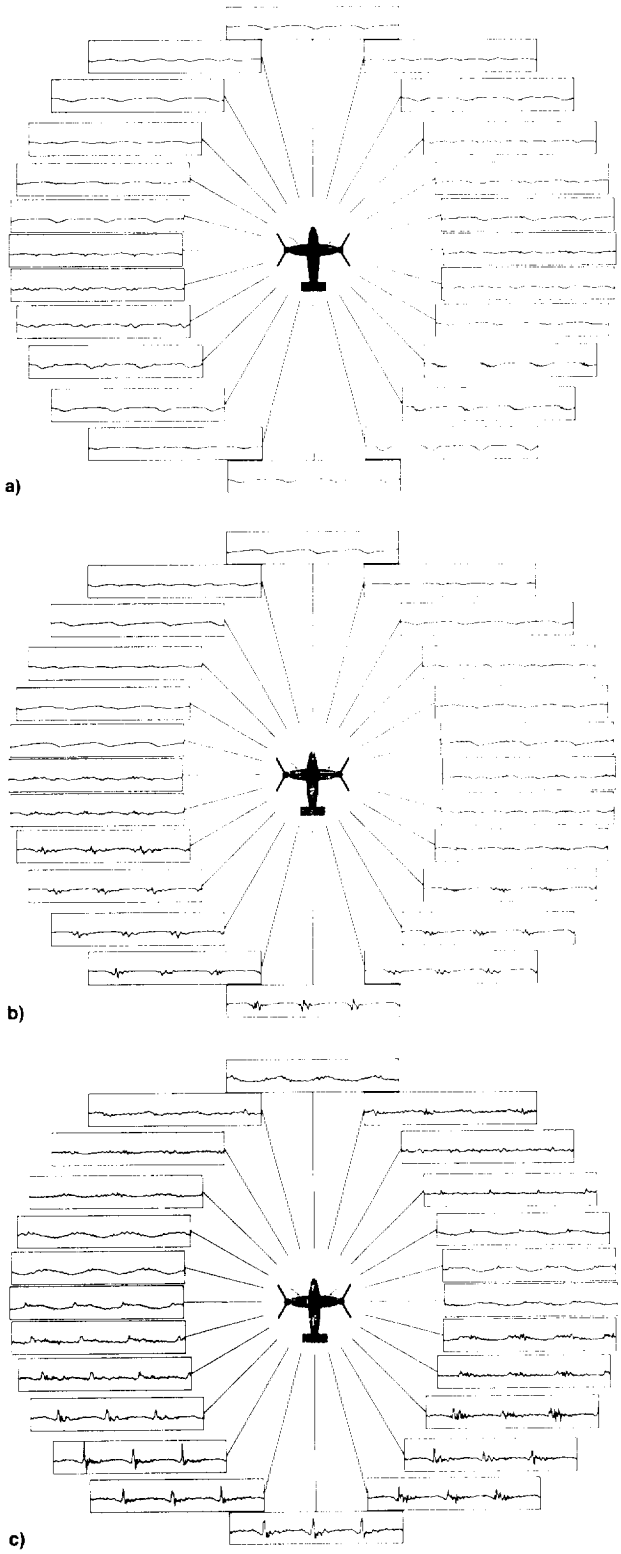


**Fig. 9 Pressure time histories; $V_T$ = 771 ft/s: $\theta$ = a) 1.6, b) 12.6, and c) 45.7 deg.**

tip path plane, at the maximum rotor tip speed of 771 ft/s and a gross weight range of 13,000 to 13,500 lb, are presented in Figs. 10 and 11, respectively. All data were corrected to a range of 715 ft and the resulting spherical surface was mapped onto the disk of the figure. A simple linear interpolation was used between measurement locations. Figure 10 shows that the highest OASPLs generally occurred on or near the aircraft axis directly fore and aft of the aircraft and to the sides just forward of $\Psi$ = 90 and 270 deg. A maximum OASPL of approximately 100 dB occurred aft of the aircraft at $\Psi$ = 0

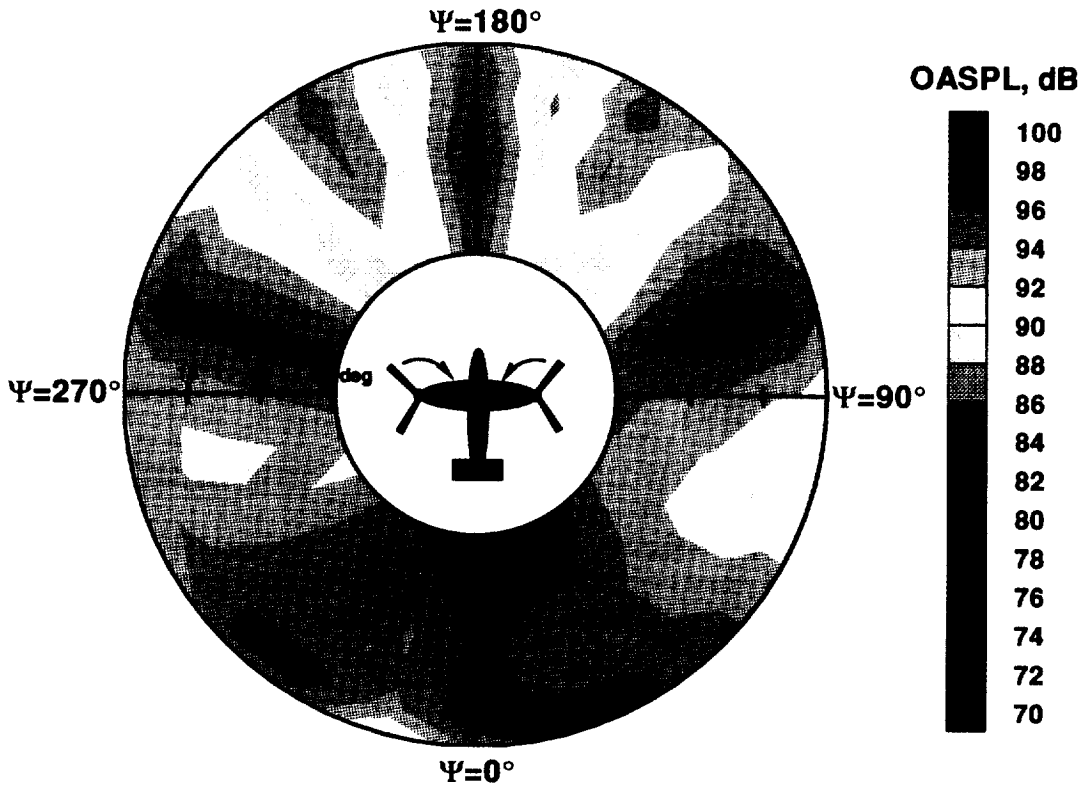


Fig. 10 OASPL contours; $V_T$ = 771 ft/s, effective microphone distance = 715 ft.

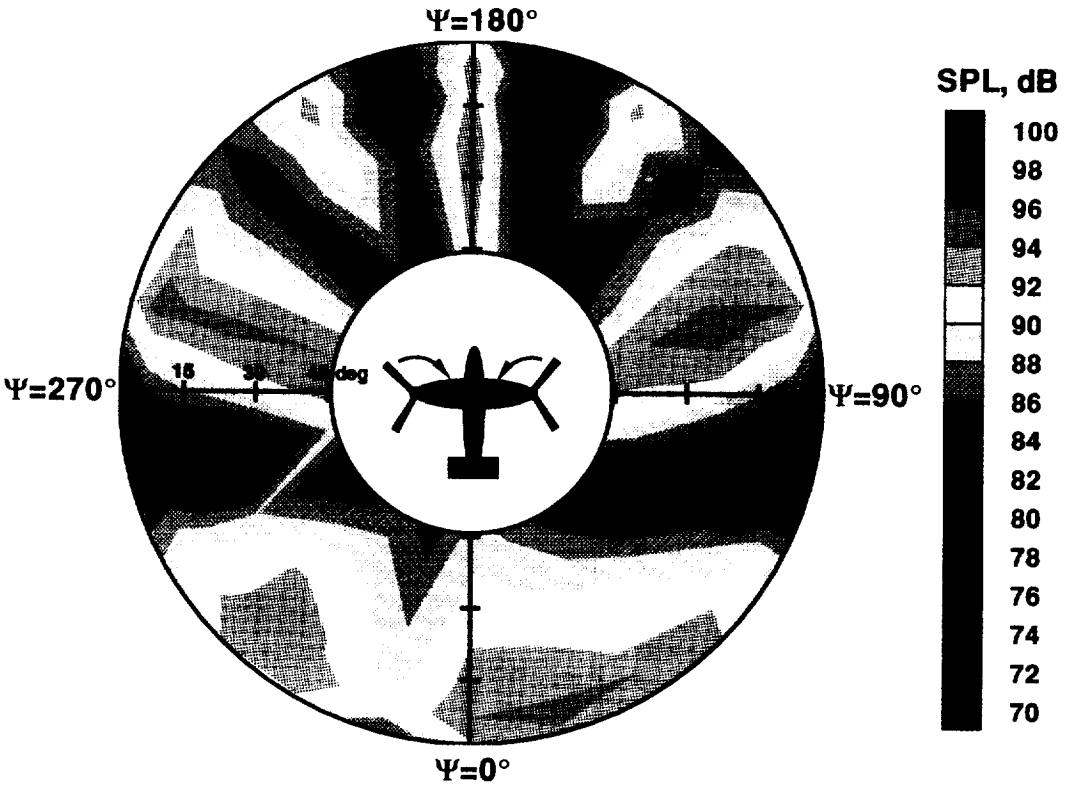


Fig. 11 SPL contours of fundamental BPF; $V_T$ = 771 ft/s, effective microphone distance = 715 ft.

deg between 40–45 deg below the rotor plane. Overall levels in the rear quadrants were higher than in the forward quadrants, probably due to the interaction of the rotors with the turbulent fountain flow. Minimum OASPLs of less than 90 dB occurred in much of the front quadrants and in a small pocket to the starboard side of the aircraft at Ψ = 75 deg between 10–15 deg below the rotor plane. The modest noise levels which propagate from the aircraft near in-plane indicate that thickness noise, which can dominate in-plane noise levels, is not a major contributor to the overall noise levels emitted by this aircraft when operating in hover.

The lower hemispherical contour plot of the fundamental BPF presented in Fig. 11 shows similar trends as were seen for the OASPL of Fig. 10, with the exception that the sound pressure levels are reduced and the area of high levels aft of and near 45 deg beneath the rotor does not exist. The max-

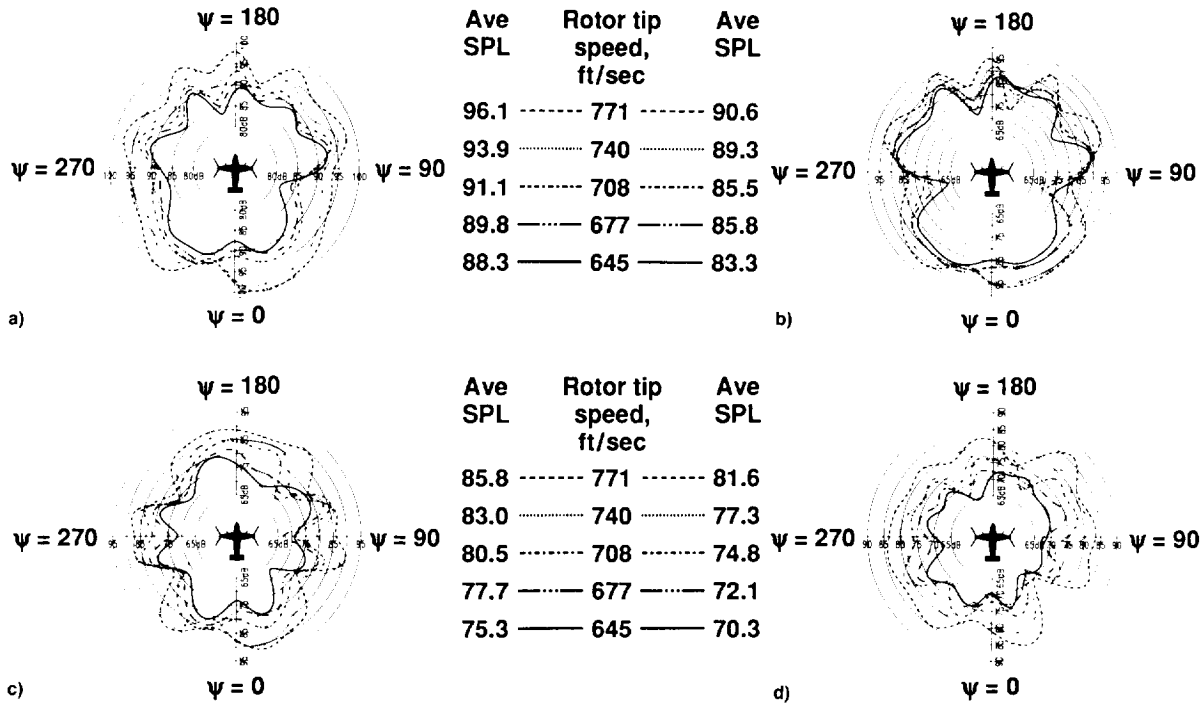


Fig. 12 Effect of $V_T$ on SPL at $\theta$ = 1.6 deg: a) OASPL, b) fundamental BPF, c) 1st harmonic of BPF, and d) 2nd harmonic of BPF.

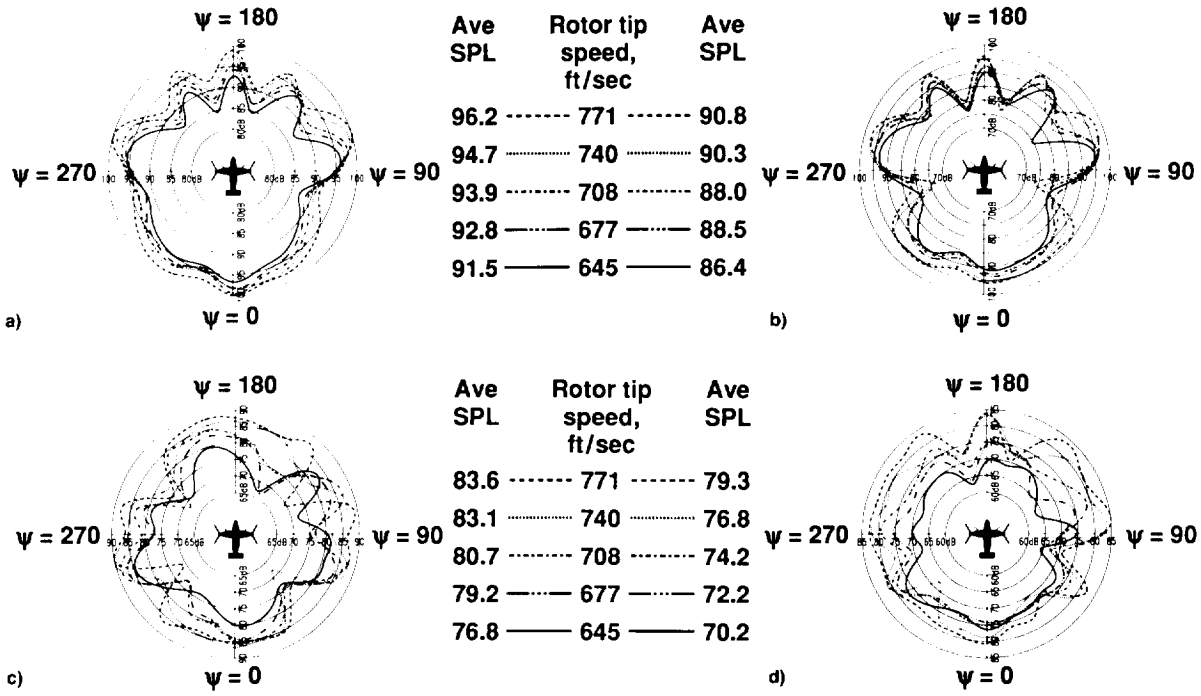


Fig. 13 Effect of $V_T$ on SPL at $\theta$ = 12.6 deg: a) OASPL, b) fundamental BPF, c) 1st harmonic of BPF, and d) 2nd harmonic of BPF.

imum SPL was about 95 dB and occurred in the forward quadrants at $\Psi$ = 105, 180, and 255 deg. Similar levels were measured in the aft quadrants between $\Psi$ = 300–60 deg from near in-plane to about 20 deg below the rotor plane.

#### Effects of Rotor Tip Speed

The effects of rotor tip speed on the OASPL and the SPL of the fundamental BPF and the first two harmonics are presented as functions of azimuth angle in Fig. 12 for $\theta$ = 1.6 deg, and in Fig. 13 for $\theta$ = 12.6 deg. The rotor tip speed range was 645–771 ft/s. The data of this figure have not been corrected to a constant source-to-microphone range. The average SPLs presented in these figures are the mean levels for the 24 azimuth angle measurement locations at each rotor tip speed. Figure 12a shows that, at $\theta$ = 1.6 deg, the average OASPL increased from 88.3 dB at $V_T$ = 645 ft/s to 96.1 dB at $V_T$ = 771 ft/s, for an average increase of almost 8 dB. This increase was anticipated since in-plane rotor noise is dominated by thickness noise, which increases with rotor tip speed.[12] A maximum OASPL of approximately 100 dB occurred at $\Psi$ = 15 and 330 deg, that was probably due to the rotors interacting with the turbulent fountain flow as the blades passed over the wing. The acoustic signatures are not symmetric about the aircraft lateral or longitudinal axes and have a scal-

loped shape in the forward quadrants ($\Psi$ = 90 to 270 deg). It has been shown that this scalloped shape is caused by phase differences of as much as 180 deg between the acoustic signals from the two rotor systems at each microphone position resulting from changes in their relative source-to-microphone distances with $\Psi$.[13]

The average SPL of the fundamental blade passage frequency at $\theta$ = 1.6 deg (Fig. 12b) increased from 83.3 dB at $V_T$ = 645 ft/s to 90.6 dB at $V_T$ = 771 ft/s, or an increase of 7.3 dB. The overall shape of the noise contours and the locations of maximum SPL are very similar to that for the OASPL with the exception that nodes have developed in the forward quadrants near $\Psi$ = 90 and 270 deg where the rotor tip speed has little effect on the SPL. The maximum SPL decreases by 5 dB for each progressively higher harmonic of the fundamental BPF, whereas the locations of the maximum SPL remain relatively unchanged (Figs. 12c and 12d). The noise contours for the second harmonic of Fig. 12d exhibit significantly higher levels on the starboard side of the aircraft compared to the port side.

The level and shape of the directivity patterns for the OASPL at $\theta$ = 12.6 deg (Fig. 13a) change less with rotor tip speed than was seen at $\theta$ = 1.6 deg (Fig. 12a). For the increase in $\theta$ from 1.6 to 12.6 deg, the average OASPL for the maximum rotor tip speed of 771 ft/s remained essentially constant at 96 dB. However, for all other tip speeds, the average OASPL increased for this incremental increase in $\theta$. The difference in the average OASPL for the two $\theta$ can be seen to increase as the tip speed is decreased. The maximum increase was 3.2 dB at the lowest tip speed of 645 ft/s. The maximum OASPL also remained constant at 100 dB, however, the locations of the maximum OASPL have shifted to $\Psi$ = 0, 110, and 250 deg, and the maximum levels in the forward quadrants have increased by 1–3 dB compared to the data at $\theta$ = 1.6 deg. Rotor tip speed reductions had little effect on the OASPL around $\Psi$ = 90 and 270 deg, and the noise levels were somewhat higher in the rear port quadrant as compared to the rear starboard quadrant. The fundamental BPF and the first two harmonics for $\theta$ = 12.6 deg (Figs. 13b–13d) exhibit the same trends as seen at $\theta$ = 1.6 deg, with the exception that the maximum levels generally occurred in the forward quadrants.

In summary, a reduction in rotor tip speed from 771 to 645 ft/s reduced the average OASPL by 7.8 dB at $\theta$ = 1.6 deg, and by 4.7 dB at $\theta$ = 12.6 deg. Lateral directivity varies with $\Psi$, suggesting that the acoustic signals from the two rotor systems are combining constructively and destructively due to phase differences between the two signals caused by their relative rotor-to-microphone distance, which varies with $\Psi$.

## Conclusions

An extensive, high-quality, far-field acoustics data base has been obtained for the XV-15 with advanced technology blades operating in hover. Data were obtained for a rotor tip speed range of 645–771 ft/s, an altitude range of 2–500 ft, and a gross weight range of 13,000–14,000 lb. A 12-microphone, 500-ft radius semicircular array combined with two aircraft headings provided acoustic data over the full 360-deg azimuth about the aircraft with a resolution of 15 deg. Altitude variations provided data from near in-plane to 45 deg below the rotor tip path plane.

An investigation of rotor tip speed reductions found that a reduction in rotor tip speed from 771 to 645 ft/s reduced the average OASPL for the 24 measurement locations about the aircraft azimuth by 7.8 dB in-plane and by 4.7 dB at 12.6 deg below the rotor plane.

Acoustic directivity studies show that the directivity pattern is highly variable with azimuth angle, suggesting that the acoustic signals from the two rotor systems are combining constructively and destructively due to phase differences caused by changes in their relative rotor-to-microphone distance. The acoustic signals propagated off the port and starboard sides of the aircraft are very similar, but a significant difference exists in the signals propagated forward and aft. Sharp positive pressure pulses typical of blade-vortex interactions are present in the data acquired aft of the aircraft only, probably because of the rotors interacting with the turbulent recirculated air from the fountain flow. This impulsive noise is strongest 45 deg under the rotor at an azimuth angle of 0 deg; it decreases moving forward in azimuth on either side of the aircraft and with decreasing angle under the rotor. For the maximum rotor tip speed of 771 ft/s and a range of 715 ft, maximum OASPLs of approximately 100 dB were measured between 40–45 deg under the rotor directly aft of the aircraft at $\Psi$ = 0 deg. Larger areas of high noise levels were measured aft of the aircraft in the rear quadrants as compared to the forward quadrants. The modest OASPLs measured near in-plane indicate that thickness noise should not be a major cause of concern for this aircraft.

## References

[1]Maisel, M. D., and Harris, D. J., "Hover Tests of the XV-15 Tiltrotor Research Aircraft," AIAA Paper 81-2501, Nov. 1981.

[2]Brieger, J. T., Maisel, M. D., and Gerdes, R., "External Noise Evaluations of the XV-15 Tiltrotor Aircraft," *Proceedings of the AHS National Specialists' Meeting on Aerodynamics and Aeroacoustics* (Arlington, TX), American Helicopter Society, Alexandria, VA, 1987.

[3]Golub, R. A., Becker, L. E., Rutledge, C. K., Smith, R. A., and Conner, D. A., "Some Far-Field Acoustics Characteristics of the XV-15 Tiltrotor Aircraft," AIAA Paper 90-3971, Oct. 1990.

[4]Edwards, B. D., "External Noise of the XV-15 Tiltrotor Aircraft," NASA CR 187463, May 1991.

[5]Lee, A., and Mosher, M., "An Acoustical Study of the XV-15 Tiltrotor Research Aircraft," AIAA Paper 79-0612, March 1979.

[6]Coffen, C. D., and George, A. R., "Analysis and Prediction of Tiltrotor Hover Noise," *Proceedings of the 46th Annual Forum and Technology Display of the American Helicopter Society* (Washington, DC), American Helicopter Society, Alexandria, VA, 1990.

[7]George, A. R., Smith, C. A., Maisel, M. D., and Brieger, J. T., "Tilt Rotor Aircraft Aeroacoustics," *Proceedings of the 45th Annual Forum and Technology Display of the American Helicopter Society* (Boston, MA), American Helicopter Society, Alexandria, VA, 1989.

[8]Huston, R. J., and Golub, R. A., "Noise Considerations for Tiltrotor," AIAA Paper 89-2359, July 1989.

[9]"Tilt Rotor Research Aircraft Familiarization Document," NASA TMX-62,407, Jan. 1975.

[10]Alexander, H. R., Maisel, M. D., and Giulianetti, D. J., "The Development of Advanced Technology Blades for Tilt-Rotor Aircraft," *Vertica*, Vol. 10, Nos. 3/4, 1986, pp. 315–339.

[11]Bjorkman, W. S., and Bondi, M. J., "TRENDS: The Aeronautical Post-Test Database Management System," NASA TM-101025, Jan. 1990.

[12]Schmitz, F. H., Boxwell, D. A., and Vause, C. R., "High-Speed Helicopter Impulsive Noise," *Proceedings of the 32nd Annual National Forum of the American Helicopter Society*, American Helicopter Society, Alexandria, VA, 1976.

[13]Rutledge, C. K., Coffen, C. D., and George, A. R., "A Comparative Analysis of XV-15 Test Data and WOPWOP Predictions Incorporating the Fountain Effect," *Proceedings of the AHS/RAeS Technical Specialists Meeting on Rotorcraft Acoustics and Fluid Dynamics* (Philadelphia, PA), American Helicopter Society, Alexandria, VA, 1991.